Astronomy Reports, Vol. 44, No. 9, 2000, pp. 569–578. Translated from Astronomicheskiĭ Zhurnal, Vol. 77, No. 9, 2000, pp. 643–653.

BVRI CCD Photometry of the Peculiar Galaxies NGC 5605 and NGC 5665

B. P. Artamonov[1], Yu. Yu. Badan[1], and A. S. Gusev[1, 2]

[1]*Sternberg Astronomical Institute, Universitetskii pr. 13, Moscow, 119899 Russia*

[2]*Institute of Solid-State Physics, Russian Academy of Sciences, Chernogolovka, Moscow oblast, 142432 Russia*

Received September 6, 1999

Abstract—The paper presents the results of *BVRI* CCD photometry of the late-type peculiar galaxies NGC 5605 and NGC 5665 obtained on the 1.5-m telescope of the Maĭdanak Observatory (Uzbekistan). Regions of star formation are identified and studied. The compositions of the stellar populations in various regions of NGC 5605 and NGC 5665 are estimated using two-color diagrams. The ages of blue condensations (stellar aggregates) in the spiral arms of the galaxies are determined. It is concluded that NGC 5665 underwent an interaction with another galaxy 5×10^8 yr ago. © *2000 MAIK "Nauka/Interperiodica".*

1. GENERAL INFORMATION

The problems of galactic evolution are closely related to studies of the composition of stellar populations. Investigations of peculiar galaxies, in which the processes of star formation occur more vigorously than in ordinary galaxies, are of special interest. Young objects can form unusual spatial structures in their galaxy.

We set ourselves the task of investigating the photometric properties of the peculiar galaxies NGC 5605 and NGC 5665. In particular, we were interested in the stellar populations in various regions of the galaxies and in determining the parameters of star-formation regions in the galactic disks. This could shed light on the origins of the distorted shapes of these two galaxies. NGC 5605 (Fig. 1a) and NGC 5665 (Fig. 1b) are relatively poorly studied peculiar galaxies with complex morphologies, having local regions of enhanced brightness and signs of a bar. The main characteristics of the galaxies are presented in Table 1.

NGC 5605. *BV* surface photometry was conducted by Gamal el din *et al.* [2, 3], who determined the integrated photometric parameters of the galaxy (color, luminosity, inclination, position angle) and noted the complex dependence of the elliptical isophotes on distance from the galactic center. *BV* aperture photometry was carried out by Peterson [4] using fairly large (relative to the size of NGC 5605) apertures; the resulting integrated $B - V$ value differs from that of [2, 3] by 0.15^m (0.69^m as compared to 0.55^m).

Observations at 12–100 μm [5] do not reveal signs of activity in NGC 5605 and show it to be a relatively "quiet" galaxy at infrared wavelengths. According to the classification scheme of [6], the nucleus of NGC 5605 has type CB: there is a small disk or bulge at the center of the galaxy (i.e., the nucleus is not starlike). According to 21-cm observations, the mass of neutral hydrogen in NGC 5605 is $3.4 \times 10^9\ M_\odot$ [7].

NGC 5665. The morphological type of this galaxy remains unclear: various researchers have classified it as Sa/Sc, Sc, SABc, Sc pec, SABc pec, and even SBm pec [8–13]. According to the spiral-branch classification proposed in [14], NGC 5665 is a type IV galaxy: it has a single main spiral and fragments of several other branches. NGC 5665 is included in the catalog of peculiar galaxies of Arp (Arp 49) and in the catalog of interacting galaxies of Vorontsov–Vel'yaminov (VV 412).

Surface photometry has been carried out in the *R* [15], *H* [13], and *K* [13] filters. The data of [13] suggest the possible presence of a small bar (with radius 7″) oriented along the major axis of NGC 5665. Numerous infrared studies have been carried out at 10–100 μm [5, 8–10, 16]. According to its IR properties, NGC 5665 is a normal galaxy with signs of outbursts of star formation [16]. The radio data of [17] at 4.85 GHz also suggest the presence of powerful bursts of star formation. Giuricin *et al.* [9] classify NGC 5665 as an interacting galaxy. At the same time, NGC 5665 is not a

Table 1. Main characteristics of the galaxies

Characteristics	NGC 5605	NGC 5665
Type	SABcp [1]	SABcp [1]
m_B	12.53 [1]	12.50 [1]
$M_B^{0,i}$	−20.72	−20.10
V_0, km/s	3363 [1]	2271 [1]
R, Mpc (H_0 = 75 km/s Mpc)	44.8	32.8
D_{25}, arcmin	1.74 [1]	1.9 [1]
d_{25}, kpc	22.4	18.7
Inclination, deg	33.5 [1]	44.5 [1]
Position angle, deg	74 [2,3]	145 [1]

1063-7729/00/4409-0569$20.00

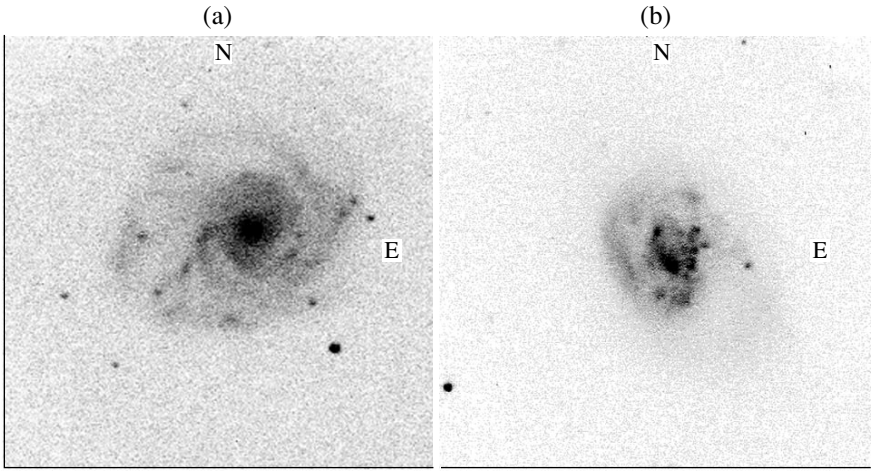

Fig. 1. CCD image of (a) NGC 5605 and (b) NGC 5665 in the *V* filter. The size of the image is $2.1' \times 2.1'$.

member of the Virgo cluster of galaxies [11] and is not perturbed by any nearby companions [18].

Spectroscopic observations of the central region of NGC 5665 at 4700–7100 Å [19] indicate that the galaxy occupies an intermediate position between LINERs (i.e., galaxies having a region of low-ionization nuclear emission) and galaxies with an abundance of HII regions (i.e., having a large number of young, hot stars). The nuclear emission type of NGC 5665 is 3.5. The galaxy is rich in gas and dust: for the total mass of NGC 5665 of $6 \times 10^{10}\ M_\odot$ derived in [12] based on 21-cm line observations, the mass of HI is about $1 \times 10^9\ M_\odot$ [10–12, 20] and the mass of dust is $M_{\rm dust} = 1.4 \times 10^7\ M_\odot$ [10].

2. OBSERVATIONS AND REDUCTION

Our observations of the two galaxies were carried out on July 6 and 7, 1997, on the 1.5-m telescope of the Sternberg Astronomical Institute (focal length 12 m) of the Maĭdanak Observatory (Uzbekistan), using the Pittsburgh University TI-800 CCD camera. The CCD camera had characteristics standard for its class. The size of the field imaged (for the 12-m focus) was 3.6′. The camera was liquid-nitrogen cooled.

Together with the receiver system, the filters used formed bands close to those of the Johnson–Cousins *BVRI* system. Information about the filters is published in [21].

We obtained CCD images of NGC 5605 and NGC 5665 in the *B*, *V*, *R*, and *I* bands (two images of each galaxy in each filter). The exposures for the *V*, *R*, and *I* filters were 2 min; the exposures for the *B* filter were 3 min, except for the second image of NGC 5605, for which the exposure was 4 min. The scale of the images during the observations was 0.25″/pixel, and the seeing was 0.7″–0.9″.

Subsequent reduction of the data was carried out on a personal computer at the Sternberg Astronomical Institute using standard procedures in the ESO–MIDAS and IRAF packages. The main stages of data reduction included:

(a) correction of the data for the amplification shift of the array and the flat field;

(b) subtraction of the sky background from each image;

(c) superposition of the galaxy images using reference stars;

(d) merging of images made in the same filters;

(e) translation of the measurements to a logarithmic scale (mag/arcsec^2);

(f) translation of the measurements from the instrumental system to the Johnson–Cousins system in accordance with color equations derived earlier in [21, 22].

The photometric ties in the *B*, *V*, *R*, and *I* filters were based on the Landolt standard stars SA110 and PG1657 + 078 [23]. The accuracy of the photometric tie was 0.07^m.

To construct the two-color diagrams, we corrected the data for Galactic absorption using the standard procedure adopted in the RC3 catalog [1]. Corrected quantities are denoted with a subscript "0."

Taking into account the known distances to the galaxies, the scales of the images were 54 pc/pixel for NGC 5605 and 36 pc/pixel for NGC 5665.

3. ANALYSIS OF RESULTS

3.1. Photometric Profiles and Morphologies of the Galaxies

NGC 5605. Figures 2a and 2b present *B*, *V*, *R*, and *I* photometric sections along the major axis of NGC 5605 (position angle 57°) passing through the galaxy's center; Figure 2c shows an isophote map in the *R* filter. The galaxy has a nucleus 1.7 kpc (8″) in diameter, which makes a smooth transition to the bulge (Figs. 2a, 2b). The diameter of the bulge is about 3 kpc (14″). At large dis-

tances from the center, the emission is dominated by the contribution of the disk.

The photometric nucleus and bulge are poorly distinguished: the photometric profile of the nucleus resembles that of the bulge, as was also noted in [6]. The maximum surface brightness at the center of the nucleus (m_B/arcsec^2 = 20.0, m_R/arcsec^2 = 18.4) is lower than the standard brightness for the nuclei of normal galaxies. This also indicates that the photometric characteristics of the nucleus of NGC 5605 are not starlike.

In the inner part of the disk, there is a nearly rectangular region 5.4 × 4.1 kpc (25″ × 19″) in size, resembling a very short bar (Fig. 2c). The mean surface brightness of this region is constant along its major axis and is 21.4 ± 0.1 m_V/arcsec^2; this value is typical of bars [24].

NGC 5605 is characterized by a rather unusual spiral pattern: the spiral arms come out from the bar at its eastern and southern ends. Each of the arms divides into two branches about 4 kpc (18″) from the center of the galaxy: one long and tightly wound and the other short and loosely wound. One or two weak spiral arms also come out of the northern end of the bar. We cannot say anything definite about the emergence of the branches from the eastern part of the bar: if a weak spiral also comes out of this region, it is superposed with the bright arm coming out of the southern part of the bar (Fig. 2c). The branches are wound into a ring 12 kpc (55″) in diameter; the center of the ring is shifted toward the west by 1.2 kpc (5″) relative to the center (nucleus) of NGC 5605 (Fig. 1a).

The unusual dependence for the ellipticity and position angle of the isophotes on distance from the center is of special interest (Figs. 3a, 3b). The circum-nuclear region has nearly circular isophotes ($e = 0.05 \pm 0.02$) oriented in position angle 75° ± 4°. The short bar ($e = 0.13 \pm 0.01$) is elongated in position angle 30°–40°. The bright, short branches emanating from the bar "turn" the galaxy 50° toward the east: the position angle 3.3 kpc (15″) from the center is 95° ± 5°. Further variations in the position angle (and, in part, the ellipticity) of the isophotes are associated with the fact that the center of the bright ring does not coincide with the center of the galaxy's nucleus. At distances $r > 30''$ from the center, the position angle of the isophotes is 76° ± 2°, and their ellipticity is 0.34 ± 0.04, increasing from the *B* to *I* images.

The eastern part of the galaxy is brighter than the western part by 0.6^m/arcsec^2 in the *V* band (21.4 ± 0.1^m/arcsec^2 as opposed to 22.0 ± 0.1^m/arcsec^2). The size of the galaxy within the 22.5^m/arcsec^2 isophotes in the *R* band is 19 × 16 kpc (88″ × 74″).

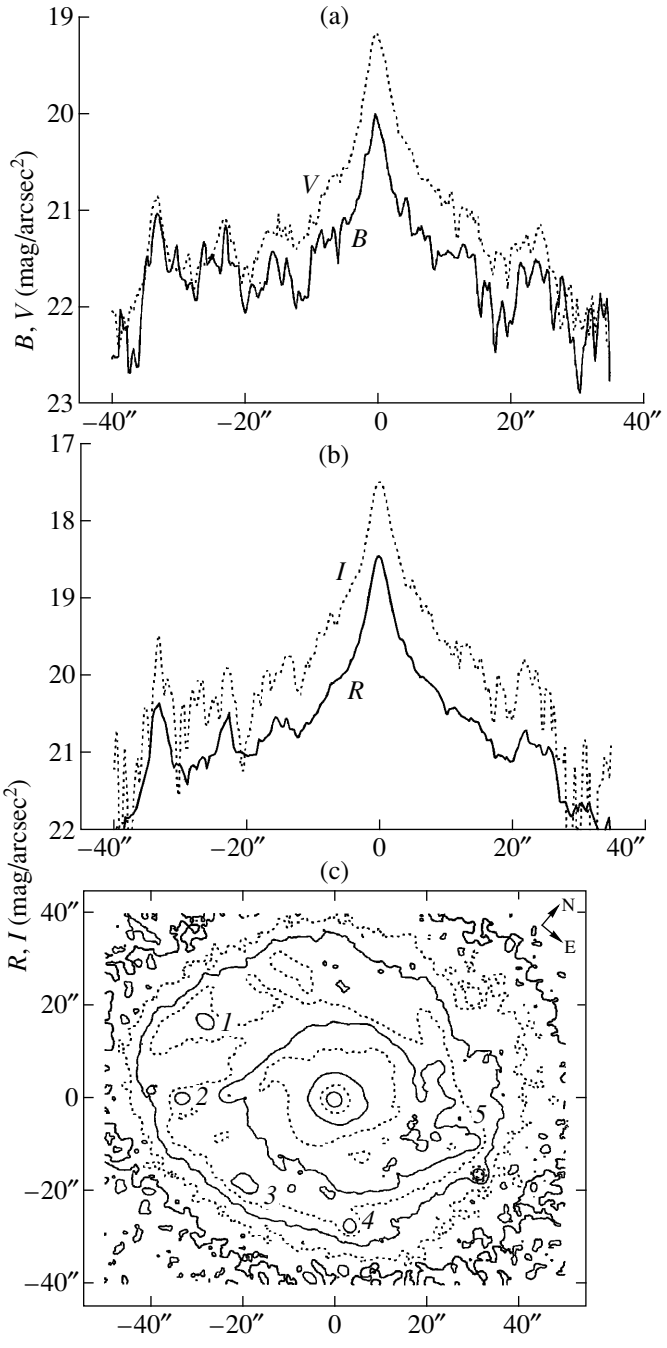

Fig. 2. Photometric profiles (mag/arcsec^2) along the major axis of NGC 5605 in the (a) *B* (solid) and *V* (dotted) and (b) *R* (solid) and *I* (dotted) filters. Panel (c) shows a contour image of the galaxy in the *R* filter (the isophotes are 19.0, 19.5, 20.0, 20.5, 21.0, 21.5, 22.0, 22.5, and 23.0). The numbers in panel (c) identify various stellar aggregates.

NGC 5665. Figures 4a and 4b present *B*, *V*, *R*, and *I* photometric sections along the major axis of NGC 5665 (position angle 138°) passing through the galaxy's center; Figure 4c presents an *R* isophote map. The galaxy is distinguished by the asymmetry of its central region along the major axis. Examining the variations of the surface brightness along the major axis toward the southeast from the center, we can make out a starlike nucleus with radius 0.43 kpc (3″) and a short bar with radius 0.85 kpc (6″), with an exponential brightness decrease along the major axis (with α^{-1} = 1.7 kpc). The surface brightness of the bar is m_V/arcsec^2 = 20.0 ± 0.2. The radius of the nucleus along the galaxy's

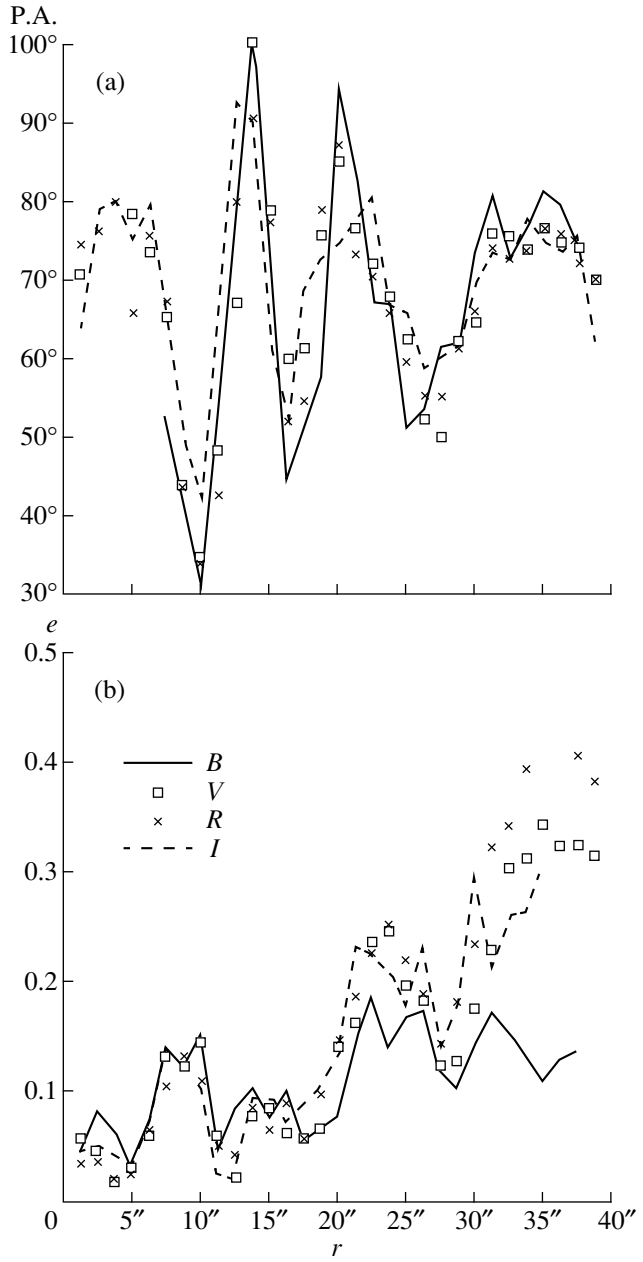

Fig. 3. Dependence of (a) position angle and (b) isophote ellipticity $e = 1 - b/a$ on distance r from the center of NGC 5605 in the B (solid), V (squares), R (asterisks), and I (dashed) filters.

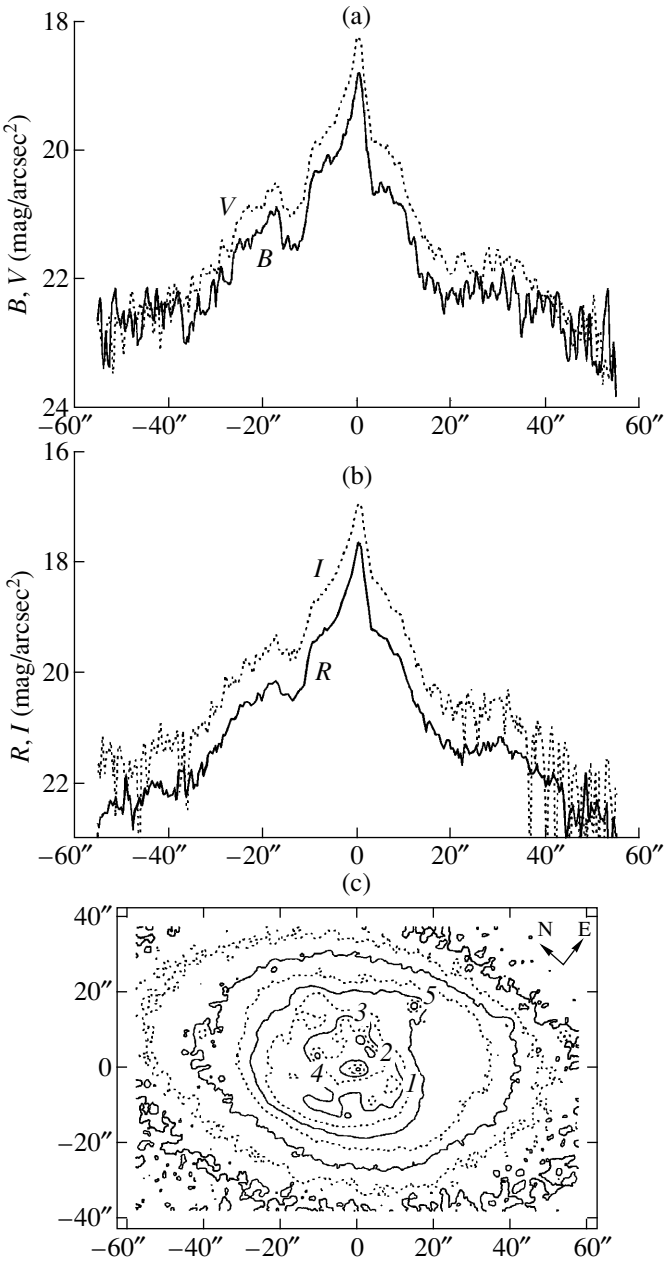

Fig. 4. Same as Fig. 2 for NGC 5665.

minor axis is also 0.43 kpc (3″; Fig. 4c). However, photometric profiles along the major axis toward the northwest from the center provide a somewhat different picture (see the left panels of Figs. 4a, 4b): the brightness fall-off within 3″ of the center corresponds not to a starlike nucleus but to a bulge. The asymmetry of the brightness distribution in the nuclear region of NGC 5665 is most clearly visible in the bluest filters (B and V). We can distinguish a bar (its northwest part) 0.58–1.15 kpc (4″–8″) from the center of the galaxy, whose R and I photometric parameters are similar to those of the southeast part of the bar.

The asymmetry of the photometric profiles in the inner regions of NGC 5665 (where the main contribution to the emission is made by the disk) is due to the fact that the sections along the major axis intersect the galaxy's spiral arms. The spiral arms are placed asymmetrically relative to the center of the galaxy and have different surface brightnesses.

The spiral pattern of NGC 5665 is extremely interesting (Figs. 1b, 4c): in addition to the two spiral branches emanating from the ends of the bar, we can see a bright, straight arm going from south to north, passing through the southeastern end of the bar. Several regions of enhanced brightness are observed in this straight arm, 250–400 pc (2″–3″) in size and with surface brightness reaching 19.1 ± 0.1^m/arcsec^2 in the *V* band. The surface brightness of the spiral arms is lower—on average, 21.0 ± 0.15 m_V/arcsec^2 and reaching 19.8 ± 0.05 m_V/arcsec^2 only in isolated places.

The position angle of NGC 5665 is $147° \pm 2°$, and the ellipticity of the isophotes is $e = 0.38 \pm 0.03$ (Figs. 5a, 5b). Based on the variation of the position angle and isophote ellipticity with distance from the galactic center, we can distinguish three regions: the central region (P.A. = $120° \pm 16°$, $e = 0.20 \pm 0.04$), the inner-disk region (P.A. = $2° \pm 2°$, *e* varies from 0.42 in the *B* image to 0.34 in the *I* image), and the outer region. The size of NGC 5665 within the 22.5^m/arcsec^2 *R* isophotes is 15.5×9.2 kpc ($107″ \times 64″$).

3.2. Color Indices

The data presented in this section have not been corrected for Galactic and internal absorption. However, we have calculated corrections associated with Galactic absorption (*E*) and the reduction of the galaxy to a "face-on" position (*E*(*i*)), calculated from RC3 data listed in Table 2.

NGC 5605. Figure 6a shows the $B - V$, $V - R$, and $R - I$ color indices along the major axis of NGC 5605, while Figures 6b–6d show color-index maps. On the whole, the galaxy becomes bluer with distance from the center, most strongly in $B - V$ (Fig. 6a). $B - V$ varies from $1.15^m \pm 0.02^m$ in the nucleus to $0.4^m \pm 0.2^m$ at the periphery of the galaxy; the corresponding indices for $V - R$ are $0.65^m \pm 0.05^m$ and $0.3^m \pm 0.2^m$ and for $R - I$ are $0.7^m \pm 0.05^m$ and $0.3^m \pm 0.4^m$, respectively.

The color indices in the bar are $B - V = 0.85^m \pm 0.15^m$, $V - R = 0.55^m \pm 0.08^m$, and $R - I = 0.65^m \pm 0.10^m$. The eastern part of the galaxy is somewhat redder than the western part. $B - V$, $V - R$, and $R - I$ in the eastern part of the disk are $0.6^m \pm 0.3^m$, $0.5^m \pm 0.1^m$, and $0.4^m \pm 0.3^m$, while, in the western part of the disk, they are $0.5^m \pm 0.3^m$, $0.4^m \pm 0.2^m$, and $0.3^m \pm 0.1^m$, respectively.

NGC 5665. Figure 7a shows the $B - V$, $V - R$, and $R - I$ color indices along the major axis of NGC 5665, while Figures 7b–7d show color-index maps. The variation of the color indices along the major axis is weak (Fig. 7a). With distance from the center, the galaxy becomes bluer in $B - V$ and $V - R$: $B - V$ varies from $0.85^m \pm 0.10^m$ in the central region to $0.55^m \pm 0.25^m$ at its periphery, and $V - R$ varies from $0.55^m \pm 0.03^m$ to $0.4^m \pm 0.15^m$ from the center to the periphery. $R - I$ remains constant along the major axis and is equal to $0.55^m \pm 0.15^m$. In the southeastern end of the bar, $B - V = 0.8^m \pm 0.1^m$, $V - R = 0.5^m \pm 0.02^m$, and $R - I = 0.6^m \pm 0.05^m$; and in the northwestern end of the bar, $B - V = 0.75^m \pm 0.03^m$, $V - R = 0.5^m \pm 0.05^m$, and $R - I = 0.55^m \pm 0.05^m$.

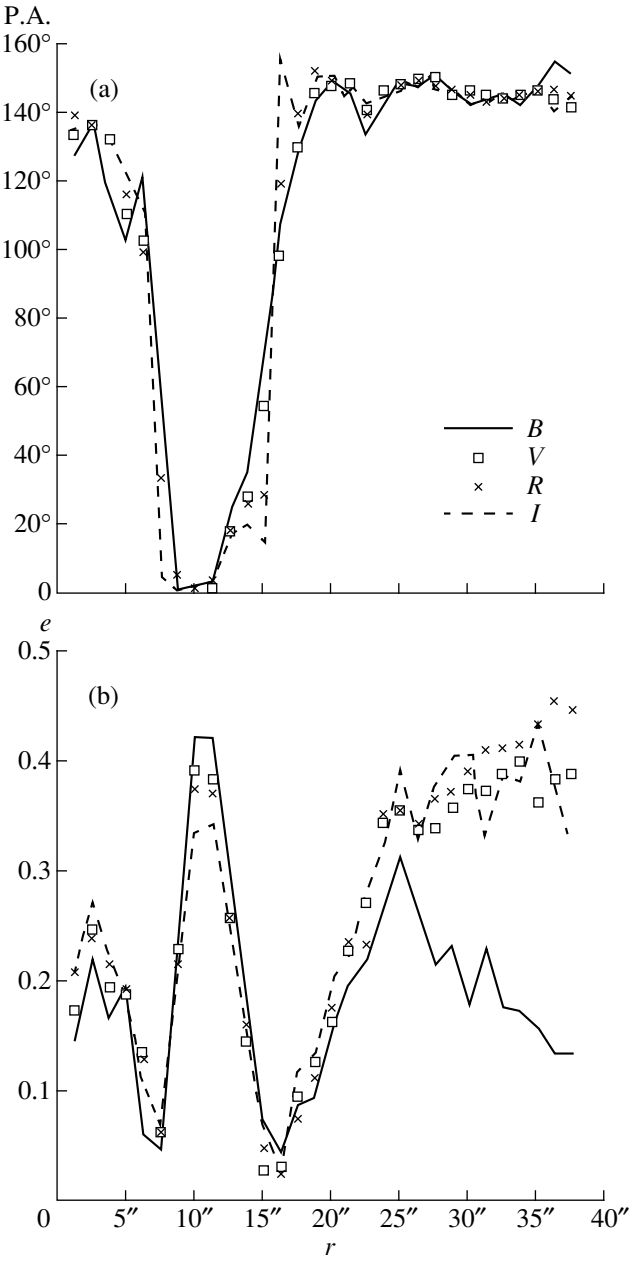

Fig. 5. Same as Fig. 3 for NGC 5665.

Overall, the distribution of colors in NGC 5665 is fairly ordinary: a red central region, blue disk between spiral arms, and still bluer spiral branches (in the branches, $B - V = 0.6^m \pm 0.1^m$, $V - R = 0.4^m \pm 0.1^m$, $R - I = 0.5^m \pm 0.1^m$). The only exception is the color distribution in the central part of NGC 5665: the region to the southeast of the nucleus is redder than the region to the northwest of the nucleus and is the reddest region in the galaxy (Figs. 7b–7d).

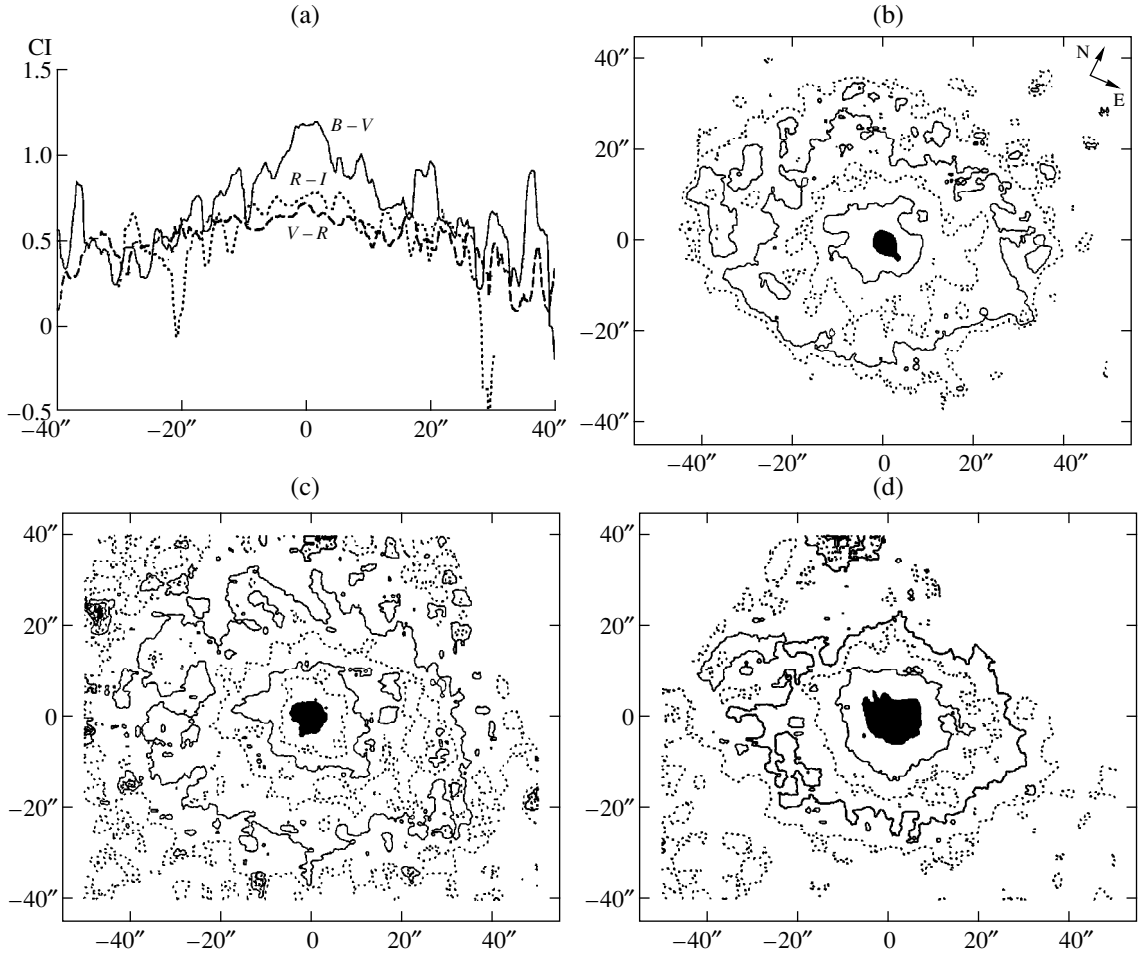

Fig. 6. (a) $B-V$ (solid), $V-R$ (dashed), and $R-I$ (dotted) color indices along the major axis of NGC 5605 and maps of (b) $B-V$, (c) $V-R$, and (d) $R-I$. The $B-V$ contours are at 0.3, 0.5, 0.7, 0.9, and 1.1, with the region with $B-V>1.1$ shaded; the $V-R$ contours are at 0.2, 0.4, 0.5, 0.55, 0.6, and 0.65, with the region with $V-R>0.65$ shaded. The $R-I$ contours are 0.0, 0.3, 0.5, 0.6, and 0.7, with the region with $R-I>0.7$ shaded.

3.3. Two-Color Diagrams

NGC 5605. Figures 8a and 8b show $(B-V)_0$–$(V-R)_0$ and $(B-V)_0$–$(V-I)_0$ two-color diagrams with all data corrected for Galactic absorption using the method proposed in RC3. The numbers in the figure indicate the colors of the (*1*) nucleus, (*2*) bulge, (*3*) disk (outside spiral branches), (*4*) spiral branches, and (*5*, *6*) bar at distances 1.7 and 2.6 kpc (8″ and 12″, respectively) from the nucleus. The squares mark the colors of five regions of enhanced brightness.

Table 2. Taking account of Galactic and internal absorption of the galaxies

Galaxy	$E(B-V)$	$E(V-R)$	$E(R-I)$
	$E_{B-V}(i)$	$E_{V-R}(i)$	$E_{R-I}(i)$
NGC 5605	0.07	0.07	0.06
	0.025	0.025	0.02
NGC 5665	0.01	0.01	0.01
	0.045	0.045	0.04

The averaging errors are $\Delta(B-V)_0 = 0.12^m$, $\Delta(V-R)_0 = 0.05^m$, and $\Delta(V-I)_0 = 0.14^m$. Most of the points in the two-color diagrams lie along the normal color sequence (NCS) for galaxies, testifying to the quiet character of the star formation in NGC 5605. An exception is certain regions of the disk and spiral branches: points *3* and *4* in Fig. 8a are shifted from the NCS. These bursts of star formation in the spiral branches and disk (between the spiral branches) are roughly equally powerful: points *3* and *4* occupy equivalent positions in the two-color diagrams within the errors. Regions of enhanced brightness in the spiral branches are not distinguished from the disk in terms of their color indices either. The characteristic size of these regions—sites of star formation—is about 450 pc (2″), corresponding to the size of stellar aggregates according to the classification of star-formation regions of Efremov [26]. Judging from its color indices, the brightest region of enhanced brightness, to the east of the center of

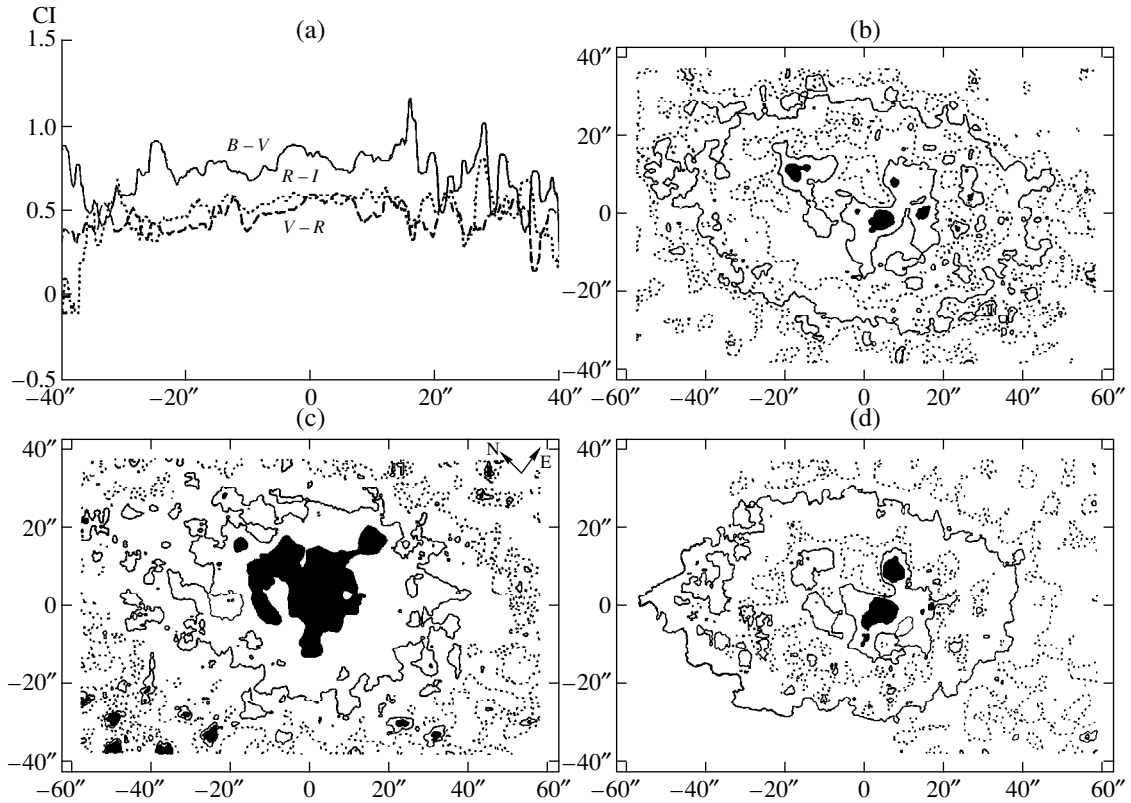

Fig. 7. (a) $B-V$ (solid), $V-R$ (dashed), and $R-I$ (dotted) color indices along the major axis of NGC 5665 and maps of (b) $B-V$, (c) $V-R$, and (d) $R-I$. The $B-V$ contours are at 0.3, 0.5, 0.7, 0.8, and 0.9, with the region with $B-V>0.9$ shaded; the $V-R$ contours are at 0.2, 0.4, and 0.5, with the region with $V-R>0.5$ shaded. The $R-I$ contours are 0.0, 0.3, 0.5, 0.55, and 0.6, with the region with $R-I>0.6$ shaded.

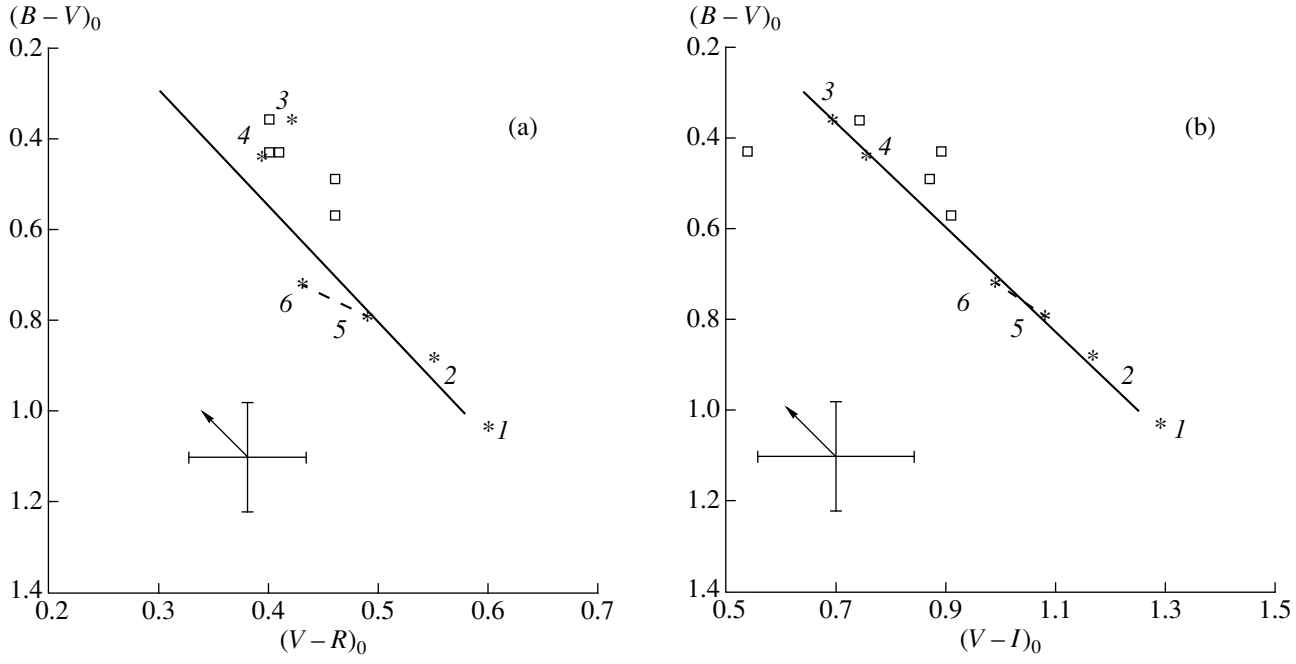

Fig. 8. (a) $(B-V)_0$–$(V-R)_0$ and (b) $(B-V)_0$–$(V-I)_0$ two-color diagrams for NGC 5605. The straight line shows the normal color sequence for galaxies from [25]. The measurement errors are indicated. The arrows show how points are shifted if internal absorption is taken into account. For other notation, see the text.

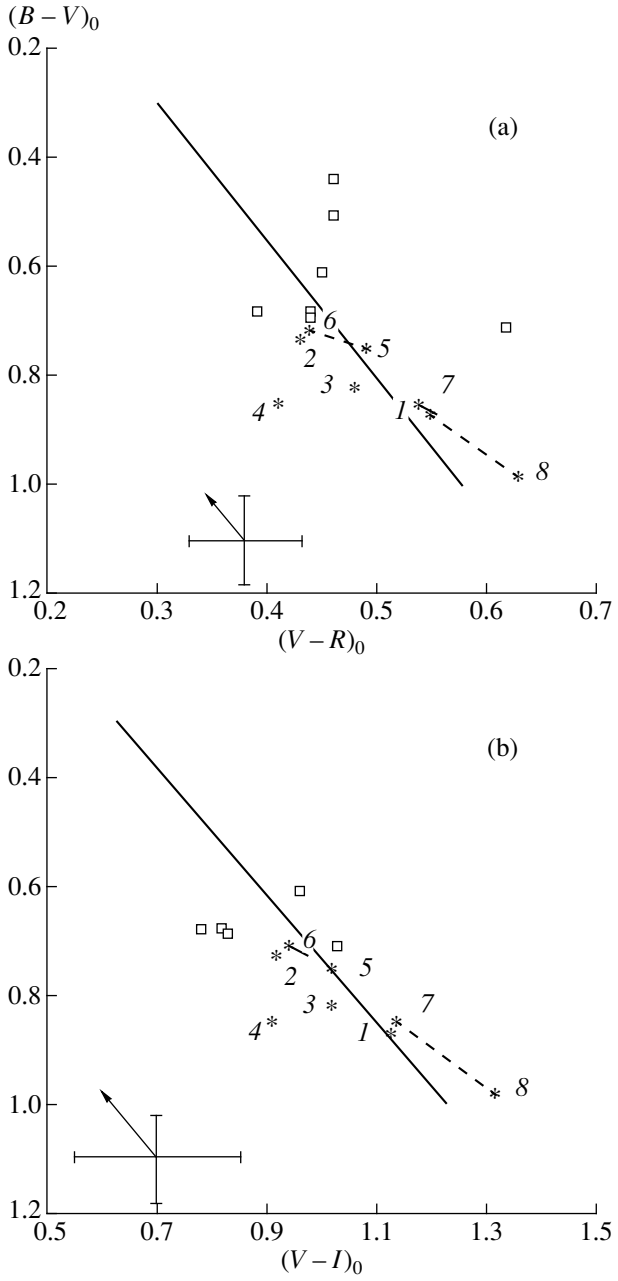

Fig. 9. Same as Fig. 8 for NGC 5665.

the galaxy (Fig. 2c), is a late F–early G star projected onto this area (the star is not shown on the two-color diagrams).

We found the star-formation rate calculated using the IR observations of [5] to be $3.3 \pm 0.2\ M_\odot$/yr and the upper limit to the star-formation efficiency to be 1×10^{-9} yr^{-1}. It is not possible to accurately determine the star-formation efficiency, since data on the mass of H_2 in the galaxy are lacking. Thus, in spite of its standard optical and IR characteristics for its morphological type, NGC 5605 is an example of a galaxy that has undergone bursts of star formation in its disk.

NGC 5665. Figures 9a and 9b show $(B-V)_0$–$(V-R)_0$ and $(B-V)_0$–$(V-I)_0$ two-color diagrams with all data corrected for Galactic absorption using the method proposed in RC3. The numbers in the figure indicate the colors of the (*1*) nucleus, (*2*) northeast spiral branch, (*3*) disk, (*4*) southwest spiral branch, (*5, 6*) northwest part of the bar at distances 5.0 and 8.5 kpc (3.5″ and 6″, respectively) from the center, and (*7, 8*) southeast part of the bar at distances 8.5 and 11.5 kpc (6″ and 8″, respectively) from the center. The squares mark the colors of five regions of enhanced brightness.

The averaging errors are $\Delta(B-V)_0 = 0.08^m$, $\Delta(V-R)_0 = 0.05^m$, and $\Delta(V-I)_0 = 0.15^m$. The points for the color indices in the central regions of NGC 5665 (the nucleus and bar) lie along the NCS, indicating that the stellar populations in these regions are standard. The positions of points *2* and *3* characterizing the northern and eastern parts of the disk (including spiral branches) correspond to a young stellar population with an age on the order of 5×10^9 yr. The color of the southwestern spiral branch (point *4*) indicates a still younger stellar component. All these factors, and also the peculiar morphology of the galaxy, suggest that NGC 5665 may have undergone a strong interaction with other galaxies in the past. The reddest region of NGC 5665 is the beginning of the visible southeastern part of the bar. The difference in the positions of the southeastern and northwestern parts of the bar in the two-color diagrams could be associated with differences in absorption by dust in these regions.

The regions of enhanced brightness in the spiral branches are the bluest regions in NGC 5665. The deviation of these regions from the NCS in the two-color diagrams (Figs. 9a, 9b) suggests the presence of outbursts of star formation. According to the classification of Efremov [26], the characteristic sizes of these sites of star formation (see Section 3.1) correspond to those of young stellar aggregates visible against the background of a relatively old disk population. We found the star-formation rate calculated using IR data to be $5.8 \pm 0.4\ M_\odot$/yr, with a high star-formation efficiency of 3.9×10^{-9} yr^{-1}.

3.4. Sites of Star Formation

Using the simulations of the color indices of stellar systems obtained in [22, 24], we determined the ages of the brightest sites of star formation/stellar aggregates in NGC 5605 and NGC 5665. In all, we studied ten such sites, five in each galaxy (Figs. 2c, 4c). Table 3 presents the main characteristics of the stellar aggregates. In contrast to the previous section and Figs. 8a, 8b, 9a, and 9b, we consider here "intrinsic" colors. We obtained the "intrinsic" intensities of the stellar aggregates by subtracting the background intensity of the spiral branches from the integrated intensity of the regions occupied by the aggregates. The first column of Table 3 gives the name of the galaxy, the second numbers identifying the aggregates, and the third to the fifth $(B-V)_{0,i}$, $(V-R)_{0,i}$, and $(V-I)_{0,i}$ color indices corrected for Galactic

absorption and internal absorption due to the inclination of the galaxy. The sixth column presents the characteristic sizes of the stellar aggregates (in pc), the seventh column gives the ages of the aggregates derived from the $(B-V)_0$–$(V-R)_0$ and $(B-V)_0$–$(V-I)_0$ two-color diagrams using the data of [24]. Note that taking into account possible additional internal absorption in the disk (not associated with the galaxy's inclination) could decrease the age of the aggregates, so that the ages in Table 3 should be considered upper limits.

The characteristic distance between the stellar aggregates in NGC 5605, taking into consideration the inclination of the disk, is 6.0 ± 0.5 kpc. The uniform distribution of the aggregates along the spiral branches is in good agreement with the theory of [26]: when protocomplexes form in the gaseous disk of a galaxy under the action of large-scale gravitational instability, the instability in the rotating gaseous disk, and especially in the spiral arms, develops most rapidly for perturbations with certain wavelengths. These wavelengths correspond to the characteristic distances between neighboring complexes (aggregates).

The stellar aggregates in NGC 5665 all have essentially the same age (except for aggregate *3*). This provides evidence for a powerful simultaneous burst of star formation in this galaxy 5×10^8 yrs ago.

4. DISCUSSION

NGC 5605. According to its photometric characteristics, this is a completely ordinary object: the central region is populated with old stars, and evidence of weak bursts of star formation is observed in the disk and spiral branches of the galaxy. The youngest regions in NGC 5605 are sites of star formation with diameters of about 450 pc—stellar aggregates with ages on the order of 10^8–10^9 yrs. The peculiarity of the galaxy is manifest only in its morphology: an asymmetric ring and the absence of a starlike nucleus. Further studies of the galaxy are required—first and foremost a map of the radial-velocity distribution. This will make it possible to determine the origin of the complex, nonstandard morphological structure of NGC 5605.

NGC 5665. A whole series of facts indicates that NGC 5665 is undergoing interaction. Its one-armed shape makes NGC 5665 resemble galaxies such as the LMC. According to [27], a one-armed structure develops when the dynamical center of the galaxy does not coincide with its center of mass. In turn, this is possible when the galaxy experiences a perturbation from another massive object. At the same time, NGC 5665 resembles Vorontsov–Vel'yaminov γ-shaped galaxies. Such γ shapes cannot form in isolated single galaxies.

The asymmetry of the brightness and colors in the circum-nuclear region of NGC 5665 (Figs. 4a–4c, 7a–7d) could also be a consequence of complex, noncentrally symmetric motions in the central regions of the galaxy. The active star formation observed in the spiral branches and the presence of a large number of sites of star formation are also characteristic of interacting galaxies. It is striking that, in single galaxies with bursts of star formation, as a rule, the sites of star formation are observed in the spiral arms in the outer parts of the disk and have a substantial range of ages (as is the case, for example, in NGC 5605); in contrast, the burst of star formation in NGC 5665 occurred in the inner eastern part of the disk, and the galaxy's stellar aggregates all have the same age (5×10^8 yrs).

Thus, overall, our photometric studies confirm the hypothesis expressed in [9]: NGC 5665 is a galaxy undergoing interaction. The absence of nearby neighbors of NGC 5665 suggests that we may be dealing with a galaxy that has swallowed a small companion. Kinematic studies of NGC 5665 are required to further test this hypothesis.

Table 3. Characteristics of stellar aggregates

NGC	No.	$(B-V)_{0,i}$	$(V-R)_{0,i}$	$(V-I)_{0,i}$	d, pc	τ, 10^8 yr
5605	1	0.72	0.38	1.06	430	7–10
	2	0.39	0.39	0.87	430	4.5–5.5
	3	0.29	0.34	0.80	430	1–2
	4	0.65	0.43	1.15	430	7–10
	5	0.46	0.23	1.02	540	3–6
5665	1	0.52	0.33	0.86	240	4.5–5.5
	2	0.56	0.23	0.73	360	4–5
	3	0.77	0.67	0.88	430	9–15
	4	0.56	0.29	0.68	400	4–5
	5	0.68	0.32	0.64	290	5–6

5. CONCLUSIONS

(1) We have identified a modestly powerful burst of star formation in the disk and spiral branches of NGC 5605. The inner region of the galaxy has a standard-age stellar population.

(2) A burst of star formation occurred in the disk of NGC 5665 5×10^8 yrs ago. It was more powerful in the southeast part of the disk than in the northwest part.

(3) The photometric characteristics of NGC 5665 suggest that this galaxy is undergoing an interaction with another galaxy.

(4) We have identified sites of star formation with sizes characteristic of stellar aggregates with ages $(1–10) \times 10^8$ yrs in NGC 5605 and $(4–5) \times 10^8$ yrs in NGC 5665.

ACKNOWLEDGMENTS

We thank A. V. Zasov for discussions of our results. This work was supported by the Russian Foundation for Basic Research (project codes 98-02-17102 and 98-02-17490).

REFERENCES

1. G. de Vaucouleurs, A. de Vaucouleurs, H. G. Corwin, *et al.*, in *Third Reference Catalogue of Bright Galaxies* (Springer, New York, 1991).
2. A. I. Gamal El Din, I. A. Issa, A. M. I. Osman, and K. Y. Kamal, Astrophys. Space Sci. **190**, 67 (1992).
3. A. I. Gamal El Din, I. A. Issa, A. M. I. Osman, and K. Y. Kamal, Astrophys. Space Sci. **190**, 89 (1992).
4. C. J. Peterson, Publ. Astron. Soc. Pac. **94** (559), 404 (1982).
5. B. Rush, M. Malkan, and L. Spinoglio, Astrophys. J., Suppl. Ser. **89**, 1 (1993).
6. S. van den Bergh, Astron. J. **110**, 613 (1995).
7. G. Theureau, L. Bottinelli, N. Goudreau-Durand, *et al.*, Astron. Astrophys., Suppl. Ser. **130**, 333 (1998).
8. N. Devereux, Astrophys. J. **323**, 91 (1987).
9. G. Giuricin, L. Tamburini, F. Mardirossian, *et al.*, Astrophys. J. **427**, 202 (1994).
10. C. Magri, Astron. J. **108**, 896 (1994).
11. C. Giovanardi, G. Helou, E. E. Salpeter, and N. Krumm, Astrophys. J. **267**, 35 (1983).
12. D. A. Hunter, J. S. Gallagher, and D. Rautenkranz, Astrophys. J., Suppl. Ser. **49**, 53 (1982).
13. S. N. Pompea and G. H. Rieke, Astrophys. J. **356**, 416 (1990).
14. D. M. Elmegreen and B. G. Elmegreen, Astrophys. J. **314**, 3 (1987).
15. P. J. Grosbol, Astron. Astrophys., Suppl. Ser. **60**, 261 (1985).
16. M. Rowan-Robinson and J. Crawford, Mon. Not. R. Astron. Soc. **238**, 523 (1989).
17. J. J. Condon, E. Anderson, and J. J. Broderick, Astron. J. **109**, 2318 (1995).
18. D. Zaritsky, R. Smith, C. Frenk, and S. D. M. White, Astrophys. J. **405**, 464 (1993).
19. O. Dahari, Astrophys. J., Suppl. Ser. **57** (4), 643 (1985).
20. T. E. Nordgren, J. N. Chengalur, E. E. Salpeter, and Y. Terzian, Astrophys. J., Suppl. Ser. **115**, 43 (1998).
21. B. P. Artamonov, Yu. Yu. Badan, V. V. Bruevich, and A. S. Gusev, Astron. Zh. **76**, 438 (1999) [Astron. Rep. **43**, 377 (1999)].
22. A. S. Gusev, Candidate's Dissertation in Physical and Mathematical Science (Moscow, 1999).
23. A. U. Landolt, Astron. J. **104**, 340 (1992).
24. A. S. Gusev, Astron. Zh. (2000) (in press).
25. R. Buta and K. L. Williams, Astron. J. **109**, 543 (1995).
26. Yu. N. Efremov, *Sites of Star Formation in Galaxies* (FM, Moscow, 1989).
27. J. Colin and E. Athanassoula, Astron. Astrophys. **214**, 99 (1989).

Translated by D. Gabuzda